

# Chapter 9

## The Effect of Rubber Hardness on the Channel Depth of the Metallic Bipolar Plates Fabricated by Rubber Pad Forming



Hossein Talebi-Ghadikolaee, Majid Elyasi, Samaneh Shahgaldi, Shahaboddin Seddighi, Mohammad Mehdi Kasaei, and Lucas F. M. da Silva

**Abstract** In this study, rubber pad forming is employed for the cost-effective production of metallic bipolar plates. To this end, a punch with parallel serpentine flow field patterns and a rubber layer is used to form SS316 bipolar plates with a thickness of 0.1 mm. The influence of forming force and rubber hardness on the channel depth of the bipolar plates is investigated. Results show a direct relationship between the channel depth and the applied force. The maximum channel depth is decreased by increasing the hardness of the rubber. However, a remarkable reduction in the rubber hardness reduces the system's performance in supplying the pressure required for forming microchannels and results in an unformed bipolar plate. Thus, to achieve a greater channel depth, the applied force and the rubber hardness should be increased accordingly.

**Keywords** PEMFC · Metallic bipolar plates · Metal forming · Rubber pad forming · Rubber hardness

---

H. Talebi-Ghadikolaee (✉)

Faculty of Mechanical Engineering, University of Kashan, Kashan, Iran  
e-mail: [h.talebi.q@kashanu.ac.ir](mailto:h.talebi.q@kashanu.ac.ir)

M. Elyasi

Mechanical Engineering Department, Babol Noshirvani University of Technology, Babol, Iran

S. Shahgaldi

Hydrogen Energy Institute, Université du Québec À Trois-Rivières (UQTR), Trois-Rivières, QC, Canada

S. Seddighi

Faculty of Mechanical Engineering, Tarbiat Modares University, Tehran, Iran

M. M. Kasaei

Institute of Science and Innovation in Mechanical and Industrial Engineering (INEGI), Porto, Portugal

Department of Mechanical Engineering, Qazvin Branch, Islamic Azad University, Qazvin, Iran

L. F. M. da Silva

Department of Mechanical Engineering, Faculty of Engineering, University of Porto, Porto, Portugal

## 9.1 Introduction

Due to the non-renewability of fossil fuels and the rate of pollutants from burning fossil fuels, the use of clean and renewable energy sources has grown in recent years. This way, Proton-exchange membrane fuel cells (PEMFCs) have attracted a lot of attention due to their efficiency, high current density, and low operating temperature. PEMFCs are made of various parts. Bipolar plates are one of the main components in PEMFCs. These plates are typically made of graphite, composite, and metallic materials (Blunk et al. 2003; Müller et al. 2006; Talebi-Ghadikolaee et al. 2022; Modanloo et al. 2021). Graphite plates have enhanced corrosion resistance and improved conductivity. However, they have poor mechanical strength and impose high manufacturing costs due to the need for machining operations. The drawbacks of graphite plates have led researchers to explore other alternatives to these plates. In the literature, sheet metals have been studied as an alternative to graphite plates due to their superior mechanical, thermal, and electrical properties (Bar-On et al. 2002). In addition to the advantages mentioned for metallic bipolar plates, and since bipolar plates build a significant part of the weight and manufacturing cost of PEMFCs, bipolar plates fabricated with sheet metal can noticeably reduce the fuel cell weight (Sopian and Daud 2006).

The flow field pattern is another variable in metallic and non-metallic bipolar plates that plays a critical role in fuel cell performance. Hence, various patterns are used as flow fields in bipolar plates. According to the study by Li and Sabir (2005), the flow field designs are categorized into four groups including pin-type, series-parallel, interdigitated, and serpentine.

Bipolar plates are made through three main methods, including molding, machining, and forming. The molding method is used to manufacture composite plates while forming and machining methods are used to build metallic bipolar plates. In addition, hydroforming (Piccininni et al. 2022), stamping (Zhang et al. 2022), roll forming (Zeinali et al. 2022), and rubber pad forming (Teng et al. 2022) are an example of forming techniques that could be used for manufacturing metallic bipolar plates. Among all the above methods, the rubber pad forming process is of great importance due to its simpler process, lower die cost, high manufacturing speed, and appropriate surface quality. These advantages have enabled the widespread use of this technique for forming metallic bipolar plates. During the forming process, the rubber layer is used to provide the pressure required for the deformation of the sheet metal. Therefore, the rubber layer characteristics can substantially influence the process.

Concerning the process variables and to enhance the quality of the manufactured products, numerous studies have investigated the feasibility of forming metallic bipolar plates by the rubber pad forming process.

Liu and Hua (2010) studied the forming of bipolar plates by rubber pad forming using the 2D simulation method. They evaluated the influence of die radius, draft angle, and rubber layer hardness. The results showed that an increase in the die radius leads to the better filling of channels and reduces the risk of rapture. Additionally,

the rubber layer hardness had no noticeable effect on stress distribution in the manufactured plates, and an increase in the draft angle mitigated the force required for forming.

Lim et al. (2013) studied a titanium plate with a thickness of 0.1 mm through the rubber layer forming process. For this purpose, a 200-ton press was used to shape the plates. In this study, the effects of punch speed, pressure applied to the assembly, rubber pad thickness, rubber pad hardness, and draft angle on the depth of the channel have been investigated. According to the results, the channel depth in the manufactured products was improved by increasing the rubber pad thickness and reducing the hardness of the rubber layer. They eventually obtained optimal values of the forming variables by considering the effect of the variables on the channel depth in the bipolar plates.

Jeong et al. (2014) investigated the effect of punch speed, the pressure applied on the assembly, rubber thickness, and rubber hardness on forming SS304 bipolar plates. The results showed that the depth of the channels is directly related to the punch speed, pressure, and rubber thickness. In addition, a reduction in the rubber hardness improved the process of forming plates. Furthermore, increasing the draft angle, especially from 10 to 20°, improved the forming condition. The depth of the channels was not significantly altered from 20 to 30°. Hence, the angle of 20° was more desirable.

Kolahdooz et al. (2017) investigate the effect of various factors in rubber pad forming of metallic bipolar plates using the integration of finite element method and design of experiment. They showed that outer corner radius, draft angle, and the friction coefficient are the most critical parameters in the forming process.

Talebi-Ghadikolaee et al. (2020) studied the rubber pad forming of metallic bipolar plater, and they proposed a reliable method for predicting the fracture onset during the plastic deformation of the sheet metal. According to their results, the finite element model together with the normalized Cockroft–Latham criterion presented the most accurate prediction of the process (plastic and fracture behavior). Rubber pad forming of Cu/Ni clad foil microchannel was investigated by Wang et al. (2022). They used a rigid convex die (RVD) and a rigid concave die (RCD) to fabricate the bipolar plates. According to their results, higher forming loads were needed in the RCD method and the stress–strain increased when the microchannel was created using the RCD method.

As mentioned above, previous studies have investigated the effect of the rubber layer on the channel depth of bipolar plates. However, given that a greater channel depth can noticeably enhance the performance and efficiency of the fuel cell assembly, it is crucial to conduct other studies to achieve greater channel depths, which is of great importance due to the low thickness (0.1 mm) of the desired plate.

Furthermore, research has reported the advantage of reducing the rubber layer hardness in increasing the depth of the channel. However, a reduction in the rubber layer's hardness will behave contrarily and reduces the channel's depth when greater channel depths are required. This problem has not been investigated in the literature.

Additionally, since the rubber layer is a process component and remarkably affects the processing costs, it is crucial to evaluate its behavior under various conditions to determine the best item for the forming process. Accordingly, this study investigates the parameters mentioned above quantitatively.

## 9.2 Methods and Procedures

### 9.2.1 Material Characterization

In this study, SS316 stainless steel sheets with a thickness of 0.1 mm were used to manufacture bipolar plates with a serpentine flow field pattern and an approximate width and length of 55 mm. In order to determine the mechanical properties of the sheet, samples have been prepared by a wire cut machine according to ASTM E8M-04. Then, the samples were tested until fracture using the SANTAM Universal Tensile Test Machine (model: STM 250) with a loading capacity of up to 25 tons. The samples and the tensile test results including the engineering and true strain–stress curves are shown in Fig. 9.1. The plastic behavior was modeled using the Swift hardening law as follows:

$$\sigma = 1215(\varepsilon + 0.04)^{0.53} \quad (9.1)$$

where  $\sigma$  is the true flow stress and  $\varepsilon$  is the true strain.

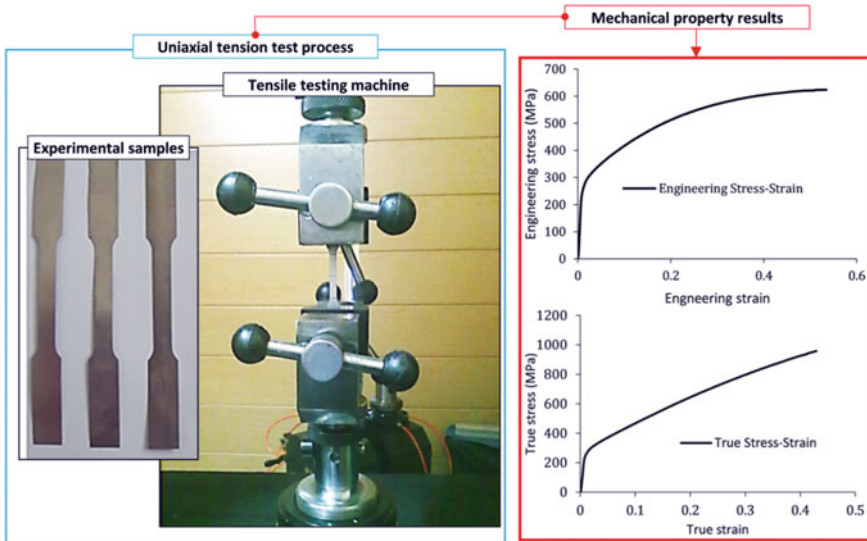


**Fig. 9.1** Uniaxial tension test procedure together with the mechanical properties results

### 9.2.2 Rubber Pad Forming Experiments

First, the required tools were fabricated to perform the rubber pad forming experiments (refer to Fig. 9.2). The punch consists of the main body and a rectangular insert made of SPK steel with a length of 100 mm and a width of 140 mm. In order to form bipolar plates, both convex and concave patterns can be utilized. In this work, the channels of the desired bipolar plate were machined in the form of convex patterns on the insert by a CNC milling machine. As shown in Fig. 9.2, the patterns created on the die have a channel width of 1.1 mm and a draft width of 1.2 mm. Furthermore, to avoid any potential rupture in the plate, the draft angle was set at 10°, and the radius of the upper and lower corners was considered to be 0.2 mm. Figure 9.2 shows the press system, the punch, and the machined patterns on the punch.

In the experiments, the rubber layer was employed as the matrix and placed in a chamber with a cavity proportional to its dimensions. The rubber layer was made from polyurethane with 60, 85, and 90 Shore A hardness while the layer thickness was constant and equal to 20 mm. A distance of 2 mm was considered between the

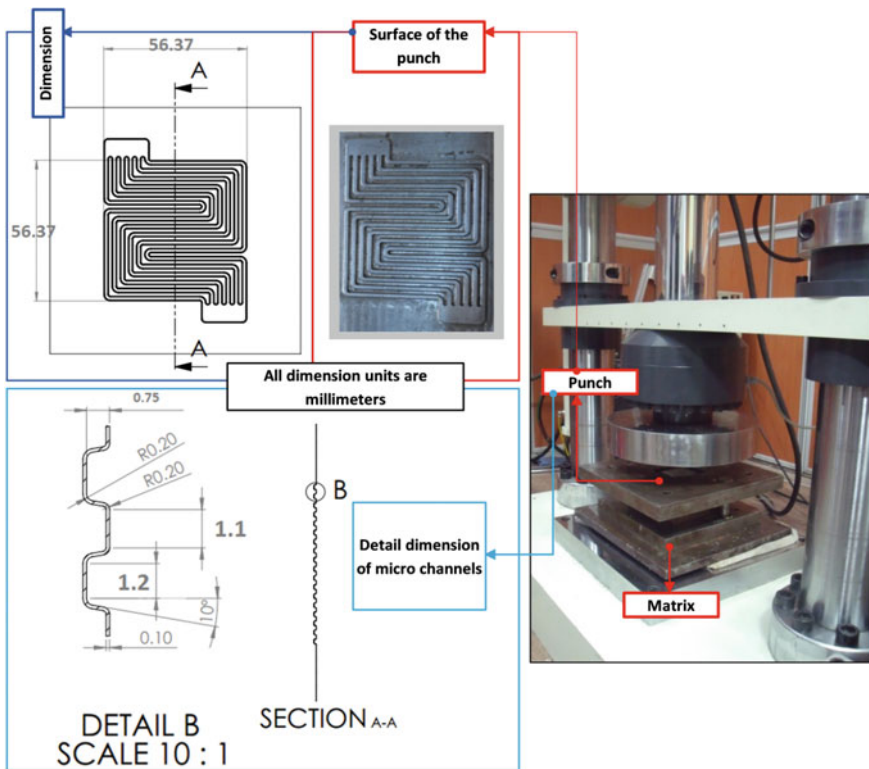


Fig. 9.2 Experimental equipment and the microchannels dimension

lateral sides of the punch and the rubber chamber (clearance) to avoid wearing the punch edge and the rubber holding chamber.

The rubber pad forming process was started by placing the sheet on the matrix. Then, the upper press jaw was driven after adjusting the desired force on the press. As a result, the rubber underwent elastic deformation and exerted pressure on the sheet to plastically deform and fill the patterns of the punch. Due to the importance of forming force and its possible relationship with the hardness of the rubber layer, specimens were formed by applying 400, 500, 800, 1000, and 1200 kN forces.

### 9.2.3 Measurement of the Channel Depth

In order to evaluate and analyze the specimens and obtain data about the channel depth of the bipolar plates fabricated under various conditions, the specimens were cut in longitudinal, transverse, and diagonal directions, as shown in Fig. 9.3. The specimens then underwent further operations to prepare the cut cross-section and enhance measurement accuracy. In addition, due to the poor quality of the specimens' cross-section after cutting by wire cut machine, the cut surfaces were molded with epoxy resin to enhance the measurement accuracy. Then, specimens were sanded and polished to enhance the quality of the cross-sections.

Afterward, an optical microscope ( $4\times$  and  $10\times$  magnification) equipped with surface measurement, and analysis software was used to measure the intended parameters. Firstly, to measure the depth of the channels, microscope images of their cross-section were taken. Then, the depth of the channels was measured by analyzing

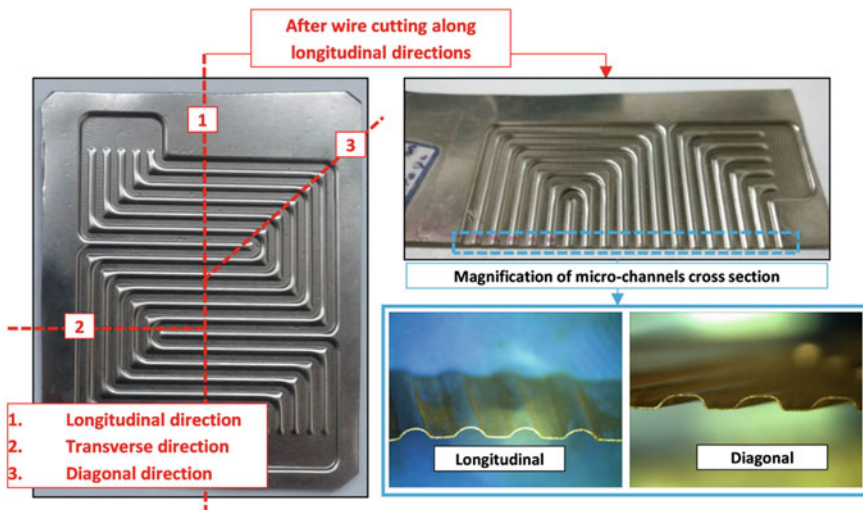


Fig. 9.3 Fabricated specimens, cutting directions together with a magnified cross-section view

images and data obtained from measuring tools embedded in the relevant software. The channel depth of the formed plates was considered as the distance between the flat zone of the specimen and the end of the dome shape area.

### 9.3 Results and Discussion

#### 9.3.1 The Effect of Applied Force on the Channel Depth

The effect of applying 400–1200 kN forces on the channel depth located in different directions of 316 stainless steel bipolar plates was investigated. For this purpose, a 20 mm-thick rubber layer with 90 Shore A was used. According to Fig. 9.4, the channel depth increases by raising the applied force. The highest channel depth in the transverse, longitudinal, and diagonal directions were 0.592, 0.568, and 0.61 mm, respectively. This occurs due to the increased deformation of the rubber layer upon increasing the force and, consequently, applying more force to the metallic plate and its higher deformation. This increase continues until the rubber layer can supply the pressure required in the chamber. The channel depth under various forces in the diagonal direction was higher than that in other directions. This is due to the larger space of the channels in this direction, which results in the easier flow of the rubber layer and thereby applying more force on the sheet. Ultimately, this leads to more deformation of the sheet and increases the channel depth. However, with the increase of the applied force, the difference between the channel depths in three directions decreases.

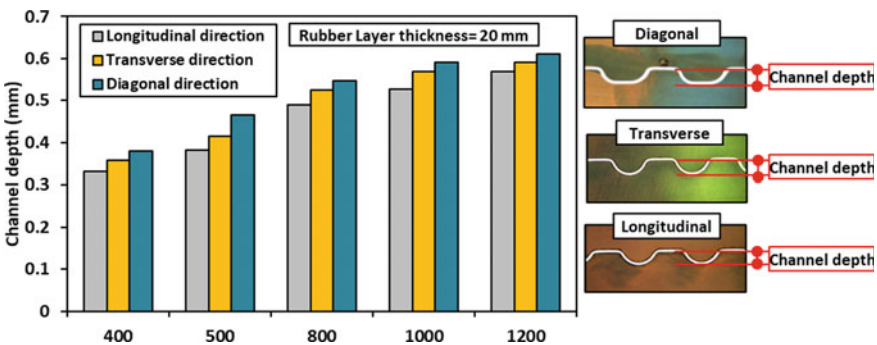


Fig. 9.4 Effect of applied force on channel depth

### 9.3.2 The Effect of Rubber Layer Hardness on the Channel Depth

Figures 9.5 and 9.6 show the results of investigating the effect of rubber hardness on the channel depth in the longitudinal and transverse directions, respectively. The results show an increase in the channel depth by decreasing rubber layer hardness at a low force of 400 kN. On the other hand, according to the observations, rubbers with low hardness slide from the space between the rubber layer chamber and the punch. This results in a considerable deformation of this region and the collapse of the rubber layer. In fact, this phenomenon avoids supplying the pressure required for forming by the rubber layer. Hence, the rubber layer with 60 Shore A cannot supply the pressure required in the chamber under the applied force of 800 kN. As a result, the highly-deformed rubber easily slides from the space between the punch and the rubber layer chamber and cannot form desired plates. The same process occurs when using a rubber layer with 85 Shore A and the applied force of 1000 kN force, which leads to inefficiency of the rubber layer and its collapse at higher forces. For this reason, the channel depth at forces above 1000 kN in the rubber layer with 85 Shore A was set at zero.

According to Figs. 9.5 and 9.6, the maximum channel depth (0.592 mm) was obtained in the rubber layer at 90 Shore A when applying a force of 1200 kN. The same results were also obtained in the longitudinal direction (Fig. 9.6). In this direction, the maximum channel depth (0.568 mm) was observed in the rubber layer at 90 Shore A when applying a force of 1200 kN.

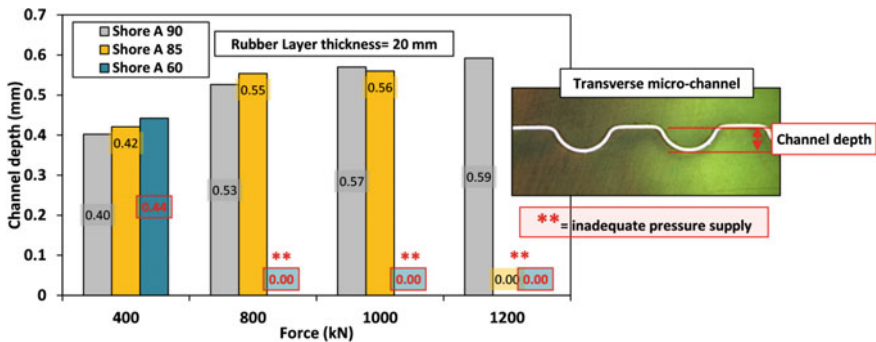


Fig. 9.5 Effect of rubber hardness on the channel depth in the transverse direction



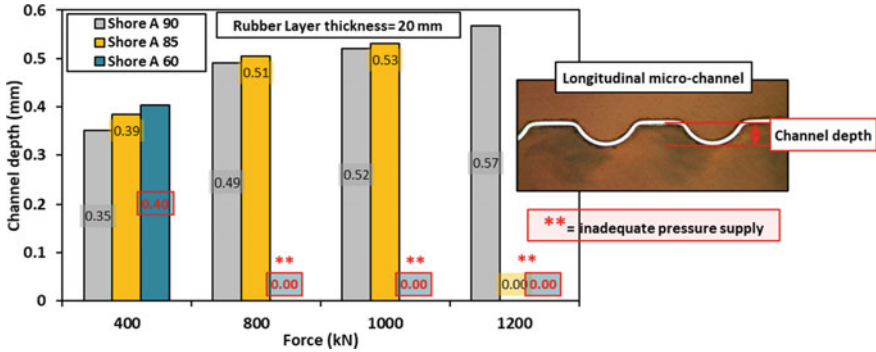


Fig. 9.6 Effect of rubber hardness on the channel depth in the longitudinal direction

### 9.3.3 Rupture Criterion

One of the most important parameters involved in the forming of metallic bipolar plates is predicting a rupture in the plate, which varies depending on the materials and their properties. Choosing a proper rupture criterion that agrees well with the experimental results can help to select an appropriate sheet metal to avoid any possible rupture. In this study, the “maximum thinning” parameter was employed to investigate rupture. The maximum thinning is determined using Eq. 9.2.

$$\text{Thinning} = \frac{t_0 - t_f}{t_0} \tag{9.2}$$

where  $t_0$  is the plate’s initial thickness. The final thickness ( $t_f$ ) is obtained from Eq. 9.3.

$$t_f = t_0 \exp(\epsilon_t) \tag{9.3}$$

On the other hand, the major engineering strain ( $e_\theta$ ) under the plane strain conditions is estimated by the empirical equation proposed by the North American Deep Drawing Research Group (NADDRG) according to Eq. 9.4:

$$e_\theta = \frac{\left[ \left( 23.3 + \frac{360}{25.4} t_0 \right) \left( \frac{n}{0.21} \right) \right]}{100} \tag{9.4}$$

where  $n$  is the strain hardening and  $t_0$  is the initial thickness of the sheet. On the other hand, under the plane strain condition, the major true strain and the thickness strain  $\epsilon_t$  can be obtained from Eqs. 9.5 and 9.6.

$$\epsilon_\theta = \ln(1 + e_\theta) \tag{9.5}$$

$$\varepsilon_t = -\varepsilon_\theta \quad (9.6)$$

The value  $t_f$  is obtained according to Eqs. 9.4–9.6 and calculating  $\varepsilon_t$  and then substituting it in Eq. 9.3. Then, the maximum thinning is obtained from Eq. 9.2. Concerning the above steps and calculations, the maximum thinning for SS316 sheet metal was estimated at 37%. To assess the accuracy of the results of the criterion utilized to determine rupture, specimens that were exposed to rupture in the experiments were employed. For this purpose, the thickness of the formed bipolar plate was measured in the regions adjacent to the rupture area. The minimum measurable thicknesses in the mentioned area were obtained, and their mean value (0.66 mm) was calculated as the minimum measurable thickness. In this study, the experimental thinning limit value was determined equal to 34% indicating a 3% error compared to the value determined by the proposed criteria (37%). The results indicate the compatibility of the experimental results with the criterion used for predicting rupture.

Accordingly, based on the results of the utilized rupture criterion, the strain hardening of the plates should exceed 0.53 to achieve thicknesses less than 0.66 mm (higher channel depth) without any rupture in fabricated microchannels.

## 9.4 Conclusions

In this study, the feasibility of forming SS316 bipolar plates with a thickness of 0.1 mm by the rubber pad forming process for use in PEMFCs was investigated. For this purpose, the effect of process variables, including force and rubber layer hardness, on the channel depth of the bipolar plates, which is among the factors affecting fuel cell performance and efficiency, was investigated.

The results showed the filling of the microchannels in the diagonal direction was higher than that in the other two directions. This was due to the larger channel space in this direction and the easier flow of the rubber layer. It was also found that at the applied force of 400 kN, harder rubbers are less efficient than softer rubbers in terms of channel depth. Nonetheless, at forces above 400 kN, softer rubbers are poorly efficient, while harder rubbers can supply the pressure required for forming the sheet, and therefore, the channel depth is increased by applying higher forces. For these reasons, the maximum channel depth (0.61 mm) was obtained in the diagonal direction in the rubber hardness of 90 Shore A and the applied force of 1200 kN. The utilized rupture criterion based on the initial thickness and the strain hardening exponent was capable of predicting the maximum allowable thinning during the rubber pad forming of metallic bipolar plates. Thus, this criterion can be used for designing this process.

## References

- Bar-On I, Kirchain R, Roth R (2002) Technical cost analysis for PEM fuel cells. *J Power Sources* 109:71–75. [https://doi.org/10.1016/S0378-7753\(02\)00062-9](https://doi.org/10.1016/S0378-7753(02)00062-9)
- Blunk RH, Lisi DJ, Yoo YE, Tucker CL III (2003) Enhanced conductivity of fuel cell plates through controlled fiber orientation. *AIChE J* 49:18–29. <https://doi.org/10.1002/aic.690490104>
- Jeong MG, Jin CK, Hwang GW, Kang CG (2014) Formability evaluation of stainless steel bipolar plate considering draft angle of die and process parameters by rubber forming. *Int J Precis Eng Manuf* 15:913–919. <https://doi.org/10.1007/s12541-014-0417-7>
- Kolahdooz R, Asghari S, Rashid-Nadimi S, Amirfazli A (2017) Integration of finite element analysis and design of experiment for the investigation of critical factors in rubber pad forming of metallic bipolar plates for PEM fuel cells. *Int J Hydrogen Energy* 42:575–589. <https://doi.org/10.1016/j.ijhydene.2016.11.020>
- Li X, Sabir I (2005) Review of bipolar plates in PEM fuel cells: flow-field designs. *Int J Hydrogen Energy* 30:359–371. <https://doi.org/10.1016/j.ijhydene.2004.09.019>
- Lim SS, Kim YT, Kang CG (2013) Fabrication of aluminum 1050 micro-channel proton exchange membrane fuel cell bipolar plate using rubber-pad-forming process. *Int J Adv Manuf Technol* 65:231–238. <https://doi.org/10.1007/s00170-012-4162-8>
- Liu Y, Hua L (2010) Fabrication of metallic bipolar plate for proton exchange membrane fuel cells by rubber pad forming. *J Power Sources* 195:3529–3535. <https://doi.org/10.1016/j.jpowsour.2009.12.046>
- Modanloo V, Talebi-Ghadikolaee H, Alimirzaloo V, Elyasi M (2021) Fracture prediction in the stamping of titanium bipolar plate for PEM fuel cells. *Int J Hydrogen Energy* 46:5729–5739. <https://doi.org/10.1016/j.ijhydene.2020.11.088>
- Müller A, Kauranen P, Von Ganski A, Hell B (2006) Injection moulding of graphite composite bipolar plates. *J Power Sources* 154:467–471. <https://doi.org/10.1016/j.jpowsour.2005.10.096>
- Piccinnini A, Cusano A, Palumbo G, Zaheer O, Ingarao G, Fratini L (2022) Reshaping end-of-life components by sheet hydroforming: an experimental and numerical analysis. *J Mater Process Technol* 117650. <https://doi.org/10.1016/j.jmatprotec.2022.117650>
- Sopian K, Daud WRW (2006) Challenges and future developments in proton exchange membrane fuel cells. *Renewable Energy* 31:719–727. <https://doi.org/10.1016/j.renene.2005.09.003>
- Talebi-Ghadikolaee H, Elyasi M, Mirnia MJ (2020) Investigation of failure during rubber pad forming of metallic bipolar plates. *Thin-Walled Struct* 150:106671. <https://doi.org/10.1016/j.tws.2020.106671>
- Talebi-Ghadikolaee H, Ahmadi Khatir F, Seddighi S (2022) Numerical-experimental study on the thickness distribution of metallic bipolar plates for PEM fuel cells. *Iran J Hydrogen Fuel Cell* 9:1–18. <https://doi.org/10.22104/IJHFC.2021.5217.1230>
- Teng F, Wang H, Shi S, Jiang L, Sun J, Sun J, Zhang S (2022) Simulation and experimental researches on multi-plate rubber pad forming of two-step micro-channel based on different forming driving models. *Int J Adv Manuf Technol* 120:4147–4157. <https://doi.org/10.1007/s00170-022-09007-4>
- Wang C, Wang H, Wang Y, Chen G, Zhu Q, Zhang P (2022) Investigation on forming methods in rubber pad forming process used for fabricating Cu/Ni clad foil microchannel. *J Manuf Process* 76:771–785. <https://doi.org/10.1016/j.jmapro.2022.03.005>
- Zeinali MS, Naeini HM, Talebi-Ghadikolaee H, Panahizadeh V (2022) Numerical and experimental investigation of fracture in roll forming process using Lou–Huh fracture criterion. *Arab J Sci Eng* 1–12. <https://doi.org/10.1007/s13369-022-06662-3>
- Zhang P, Pereira MP, Rolfe BF, Wilkosz DE, Hodgson P, Weiss M (2022) Investigation of material failure in micro-stamping of metallic bipolar plates. *J Manuf Process* 73:54–66. <https://doi.org/10.1016/j.jmapro.2021.10.044>